The connubium between quantum mechanics and crystallography

Piero Macchi
Department of Chemistry, Materials,
Chemical Engineering, «Giulio Natta»,
Politecnico di Milano, Milano, Italy

The connubium between quantum mechanics and crystallography

1. **Historical Background:** Who, What, When, Where, Why?
   1. the atomic model and the electronic structure
   2. the chemical bonding
   3. supramolecular interactions
   4. wavefunction from experiments
   5. modelling electron charge and spin densities

2. **State of the Art**
   1. standard models and beyond
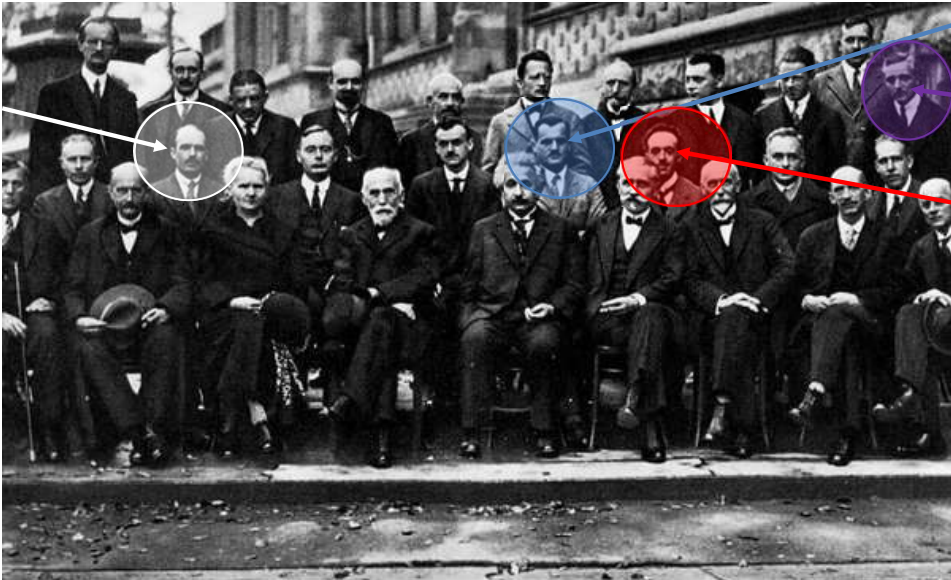   2. chemical bonding analysis
   3. molecules and beyond

POLITECNICO MILANO 1863

Historical Background

The Solvay Conference 1927: Crystallographers & Quantum Physicists

POLITECNICO MILANO 1863

SOLID SPHERE MODEL	PLUM PUDDING MODEL	NUCLEAR MODEL	PLANETARY MODEL	QUANTUM MODEL
JOHN DALTON	J.J. THOMSON	ERNEST RUTHERFORD	NIELS BOHR	ERWIN SCHRÖDINGER
1803	1897	1911	1913	1926

Rontgen 1896

Laue 1912

It seems to me that the experimental study of the scattered radiation, in particular from light atoms, should get more attention, since along this way it should be possible to determine the arrangement of the electrons in the atoms.

Debye P. Zerstreuung von Röntgenstrahlen. Ann. Phys. 1915; 351: 809–823.

The elastic scattering (Thomson)

$$\mathbf{k} \quad |\mathbf{k}| = \frac{4\pi sin\vartheta}{\lambda}$$

$\mathbf{k_0}$ photon

photon $\mathbf{k_s}$

2ϑ

electron

$$|\mathbf{k_0}| = |\mathbf{k_s}| = \frac{2\pi}{\lambda}$$

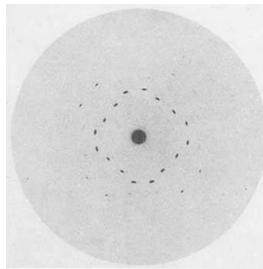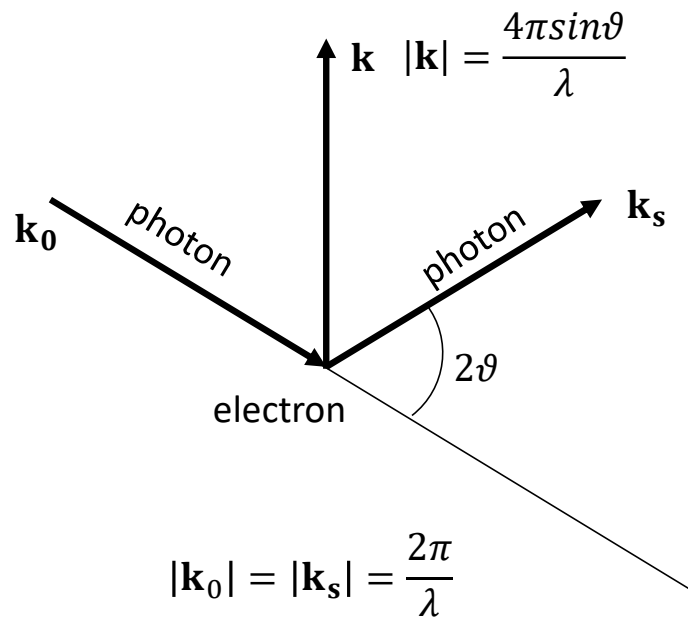A distribution which fits Bragg's data acceptably is an arrangement of the electrons in equally-spaced, concentric rings, each ring having the same number of electrons, and the diameter of the outer ring being about 0.7 of the distance between the successive planes of atoms.

Compton AH. The Distribution of the Electrons in Atoms. Nature. 1915; 95: 343-344.

ϑ ϑ

r d_{hkl}

$$n\lambda = 2d_{hkl}sin\vartheta$$
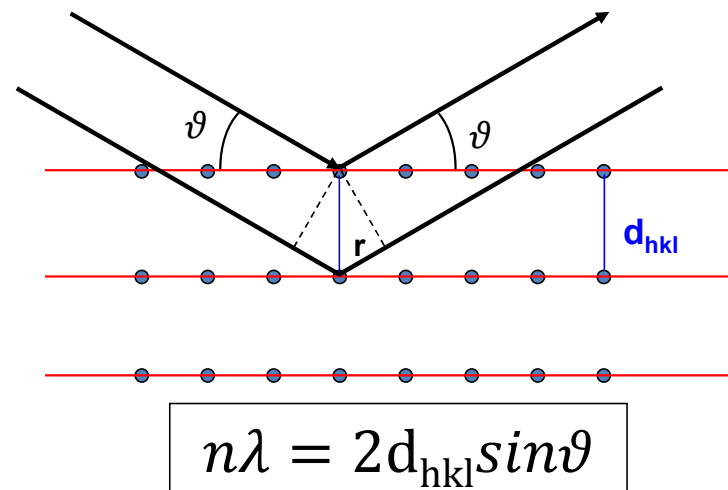
Bragg WH, Bragg WL. The Reflexion of X-rays by Crystals. Proc. R. Soc. Lond. A. 1913; 88: 428–38

POLITECNICO MILANO 1863

No second spectacular crystallographic discovery has since been made of consequences comparable with those of the original discovery of X-ray diffraction.

Ewald PP. Editorial Preface. Acta Cryst. 1948; 1: 1-2.
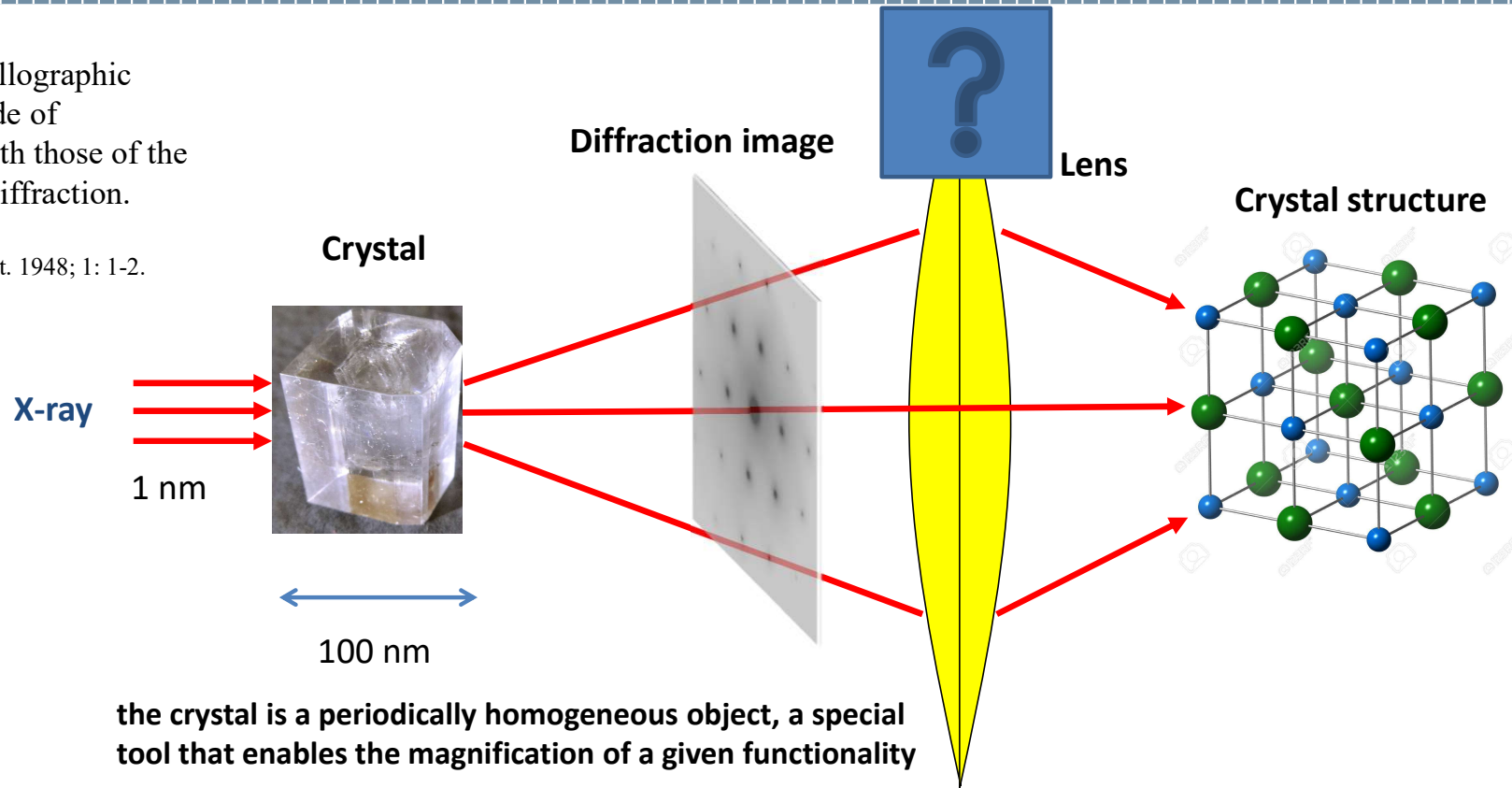
X-ray

1 nm

100 nm

Crystal

Diffraction image

Lens

Crystal structure

the crystal is a periodically homogeneous object, a special tool that enables the magnification of a given functionality

…although calculation, and not a lens, is used in the final stages of its formation, and although certain essential data, used automatically by a lens, namely the relative phases of the spectra, have to be inferred by means other than optical before the calculation can be carried out, the [Fourier] projection is nevertheless formally an optical image.
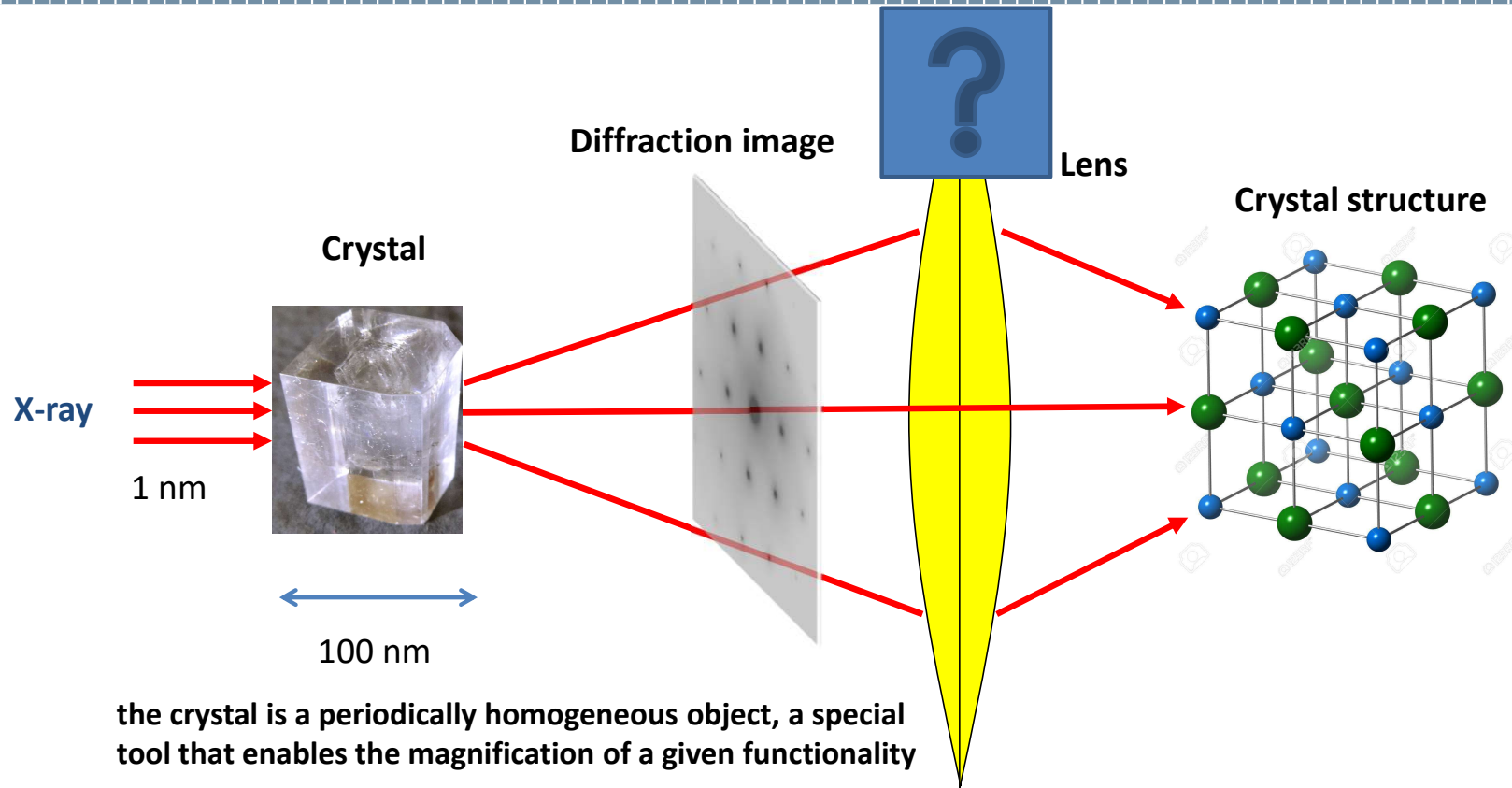
James RW. The optical principles of the diffraction of X-rays, G. Bell and Sons, London, 1958, page 385.

X-ray

1 nm

100 nm

the crystal is a periodically homogeneous object, a special tool that enables the magnification of a given functionality

Crystal

Diffraction image

?

Lens

Crystal structure
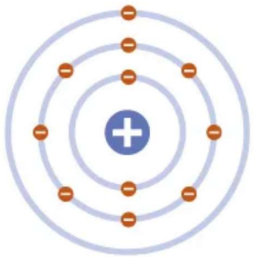
$$4\pi r^2 \rho(r)$$
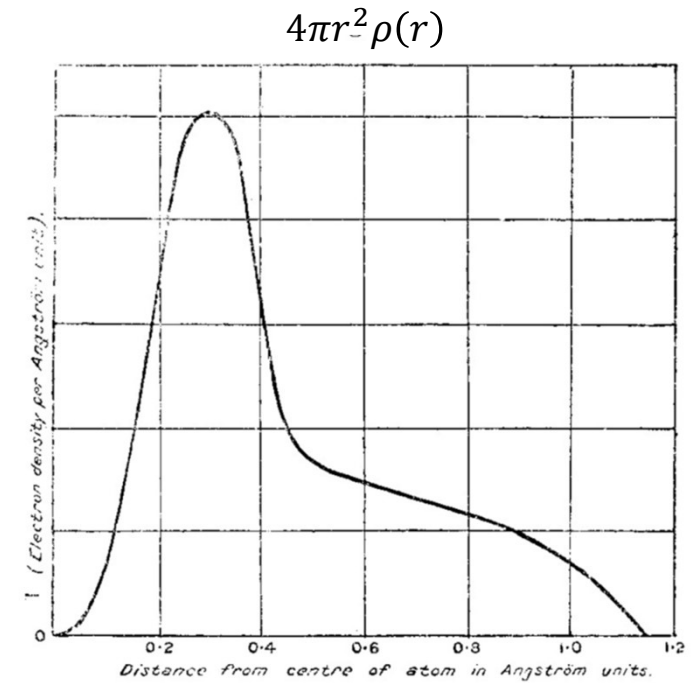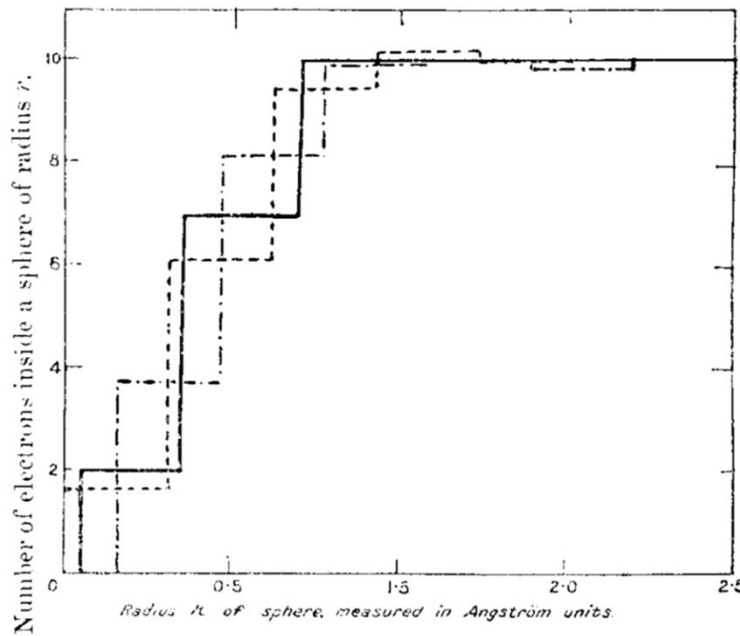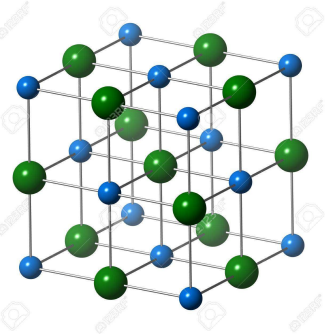
Bragg WL, James RW, Bosanquet CH.
The distributions of electrons around the nucleus in the sodium and chlorine atoms. Phil Mag. 1922; 44: 433-449.

form factor Na
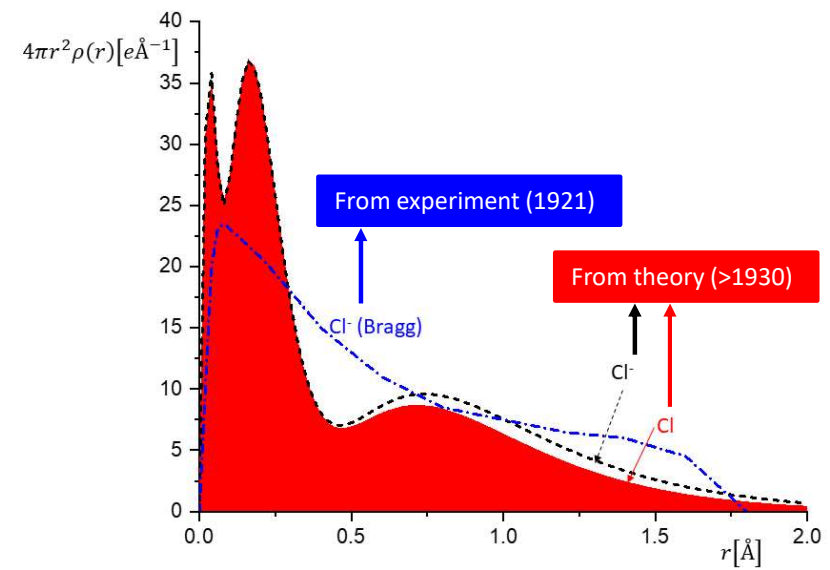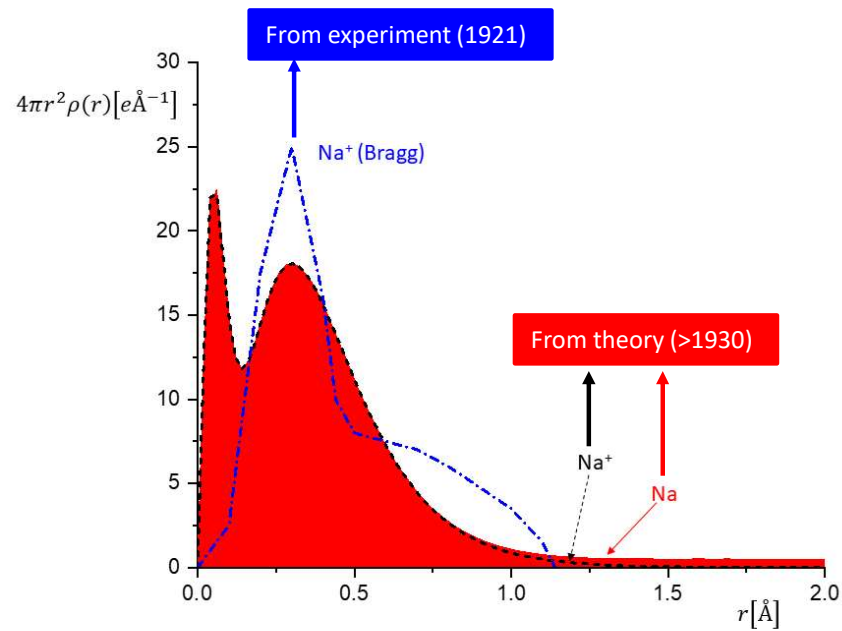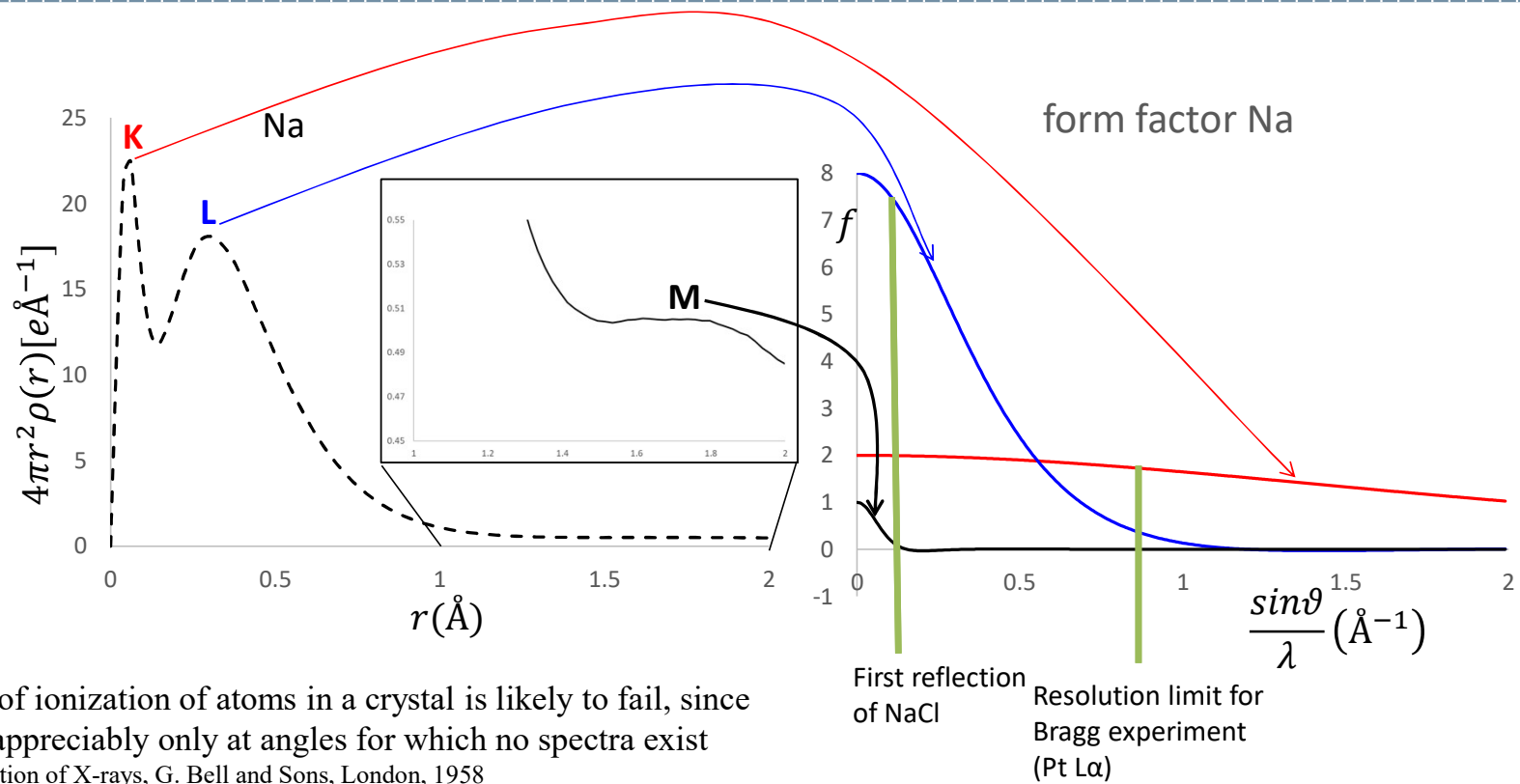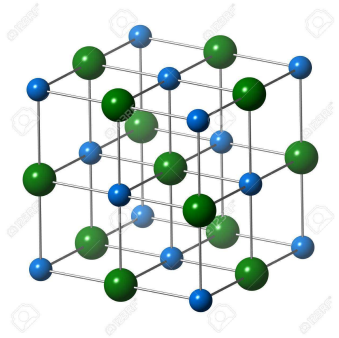
Any attempt to determine the state of ionization of atoms in a crystal is likely to fail, since scattering factor curves will differ appreciably only at angles for which no spectra exist

James RW. The optical principles of the diffraction of X-rays, G. Bell and Sons, London, 1958

First reflection of NaCl

Resolution limit for Bragg experiment (Pt Lα)

X-Ray Determination of the Number of 3d Electrons in Cu, Ni, Co, Fe, and Cr

R. J. Weiss* and J. J. DeMarco

Crystals of elemental metals are analyzed by Bragg diffraction technique to conclude that most of the valence electrons reside in 3d-states (Cu, Ni and Co) or in hybrid states (Cr and Fe).

A very difficult task, strongly affected by the so called extinction

Weiss RJ. A Physicist remembers. World Scientific Publishing Co. Pte. Ltd., Singapore, 2007.

Form factor Xe
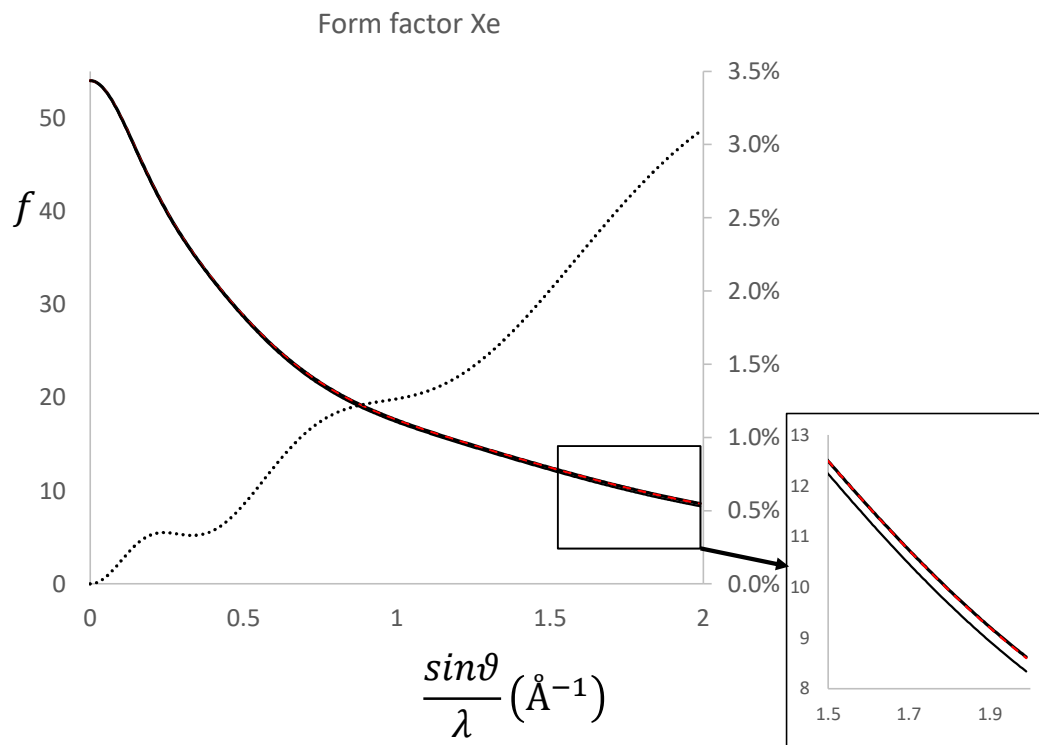
Clementi E, Roetti C. Roothaan-Hartree-Fock atomic wavefunctions: Basis functions and their coefficients for ground and certain excited states of neutral and ionized atoms, Z≤54 Atomic Data and Nuclear Data Tables. 1974; 14: 177-478. Atomic Data and Nuclear Data Tables

Roothan Hartree-Fock (non relativistic, non correlated)

Macchi P, Coppens P. Relativistic analytical wave functions and scattering factors for neutral atoms beyond Kr and for all chemically important ions up to I⁻. Acta Cryst., **2001**, A57, 656-662.

Dirac-Fock method (relativistic & correlation)

Volkov A., Macchi P. Zero-order relativistic analytical wave functions for all neutral atoms. Unpublished

Zora-Kohn-Sham method (relativistic & DFT)

- - - - - % difference between non relativistic and relativistic

POLITECNICO MILANO 1863

LOUIS DE BROGLIE

The wave nature of the electron

Nobel Lecture, December 12, 1929

For X-rays the phenomenon of diffraction by crystals was a natural consequence of the idea that X-rays are waves analogous to light and differ from it only by having a smaller wavelength. For electrons nothing similar could be foreseen as long as the electron was regarded as a simple small corpuscle. However, if the electron is assumed to be associated with a wave and the density of an electron cloud is measured by the intensity of the associated wave, then a phenomenon analogous to the Laue phenomenon ought to be expected for electrons. The electron wave will actually be diffracted intensely in the directions which can be calculated by means of the Laue-Bragg theory from the wavelength $\lambda = h/mv$, which corresponds to the known velocity v of the electrons impinging on the crystal. Since, according to our general principle, the intensity of the diffracted wave is a measure of the density of the cloud of diffracted electrons, we must expect to find a great

many diffracted electrons in the directions of the maxima. If the phenomenon actually exists it should thus provide decisive experimental proof in favour of the existence of a wave associated with the electron with wavelength h/mv, and so the fundamental idea of wave mechanics will rest on firm experimental foundations.

LIGHT IS A ~arave!
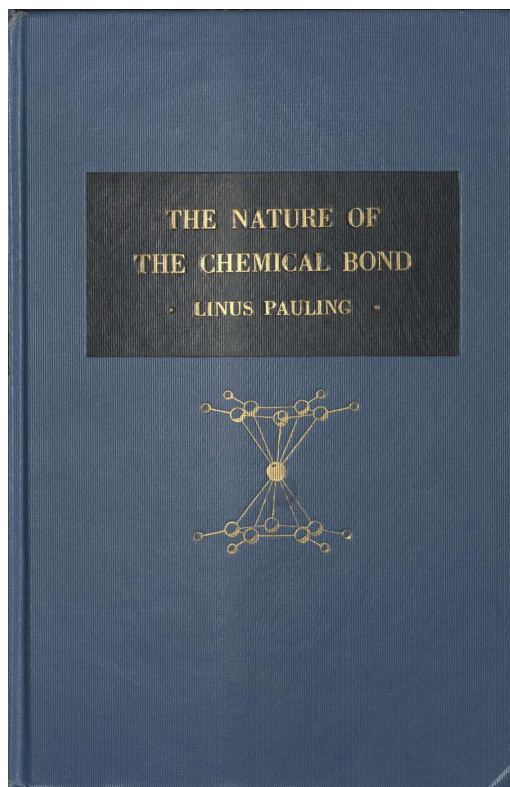
X-ray structures paved the way toward the development of modern chemical bonding theories

A small part only of the body of contributions of quantum mechanics to chemistry has been purely quantum-mechanical in character; only in a few cases, for example, have results of direct chemical interest been obtained by the accurate solution of the Schrödinger wave equation

Pauling L. The Nature of the Chemical Bonding. First edition. Cornell University Press. New York, 1939
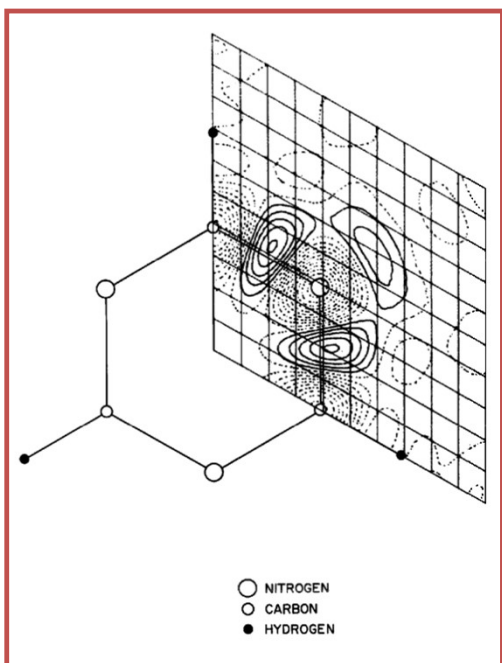
Comparative X-Ray and Neutron Diffraction Study of Bonding Effects in s-Triazine

Abstract. X-ray and neutron-diffraction data were combined for study of deviations from spherical symmetry of the atomic charge distributions in the small organic molecule s-triazine. The results indicate that density has migrated from the atomic regions into the bonds and into the nitrogen lone-pair region. Refinement procedures for x-ray data, which do not take these bonding effects into account, give parameters containing small but measurable errors.

$$\Delta\rho(\mathbf{r}) = \frac{1}{V} \sum_{|\mathbf{k}| \le k_{max}} \left(\mathbf{F}_{obs}(\mathbf{k}) - \mathbf{F}_{calc,spher}(\mathbf{k})\right) e^{i\mathbf{k}\mathbf{r}}$$

Coppens, P. (1967) *Science*, **158**, 1577–1579.

Based on a model refined from neutron diffraction

Bond Lengths, and Beyond

By Riccardo Destro and Felicita Merati

Dipartimento di Chimica Fisica ed Elettrochimica, e Centro CNR, via Golgi 19, 20133 Milano, Italy

Based on the gradient field of the electron density

$\rho(\mathbf{r})$ ← Obtained from a multipole expansion refined against X-ray diffraction data

$\nabla^2 \rho(\mathbf{r})$

BCA
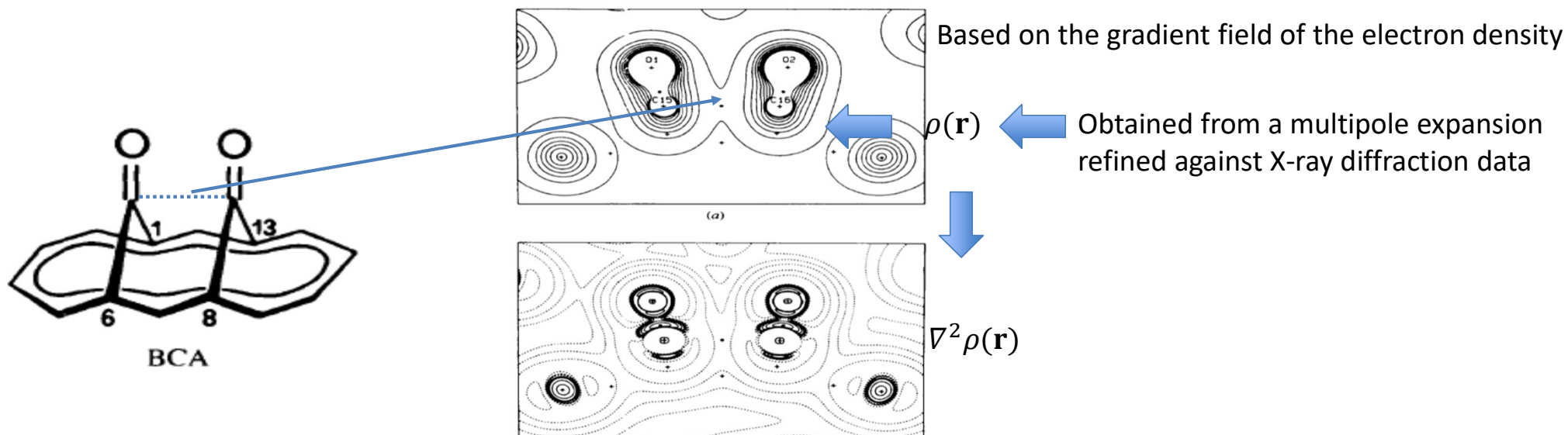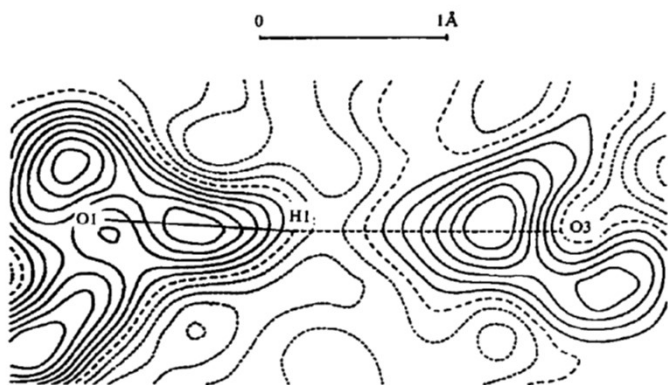
Deformation density approach

Wang Y, Tsai CJ, Liu WL. Temperature-Dependence Studies of α-Oxalic acid Dihydrate. Acta Cryst. 1985; B41:131-135
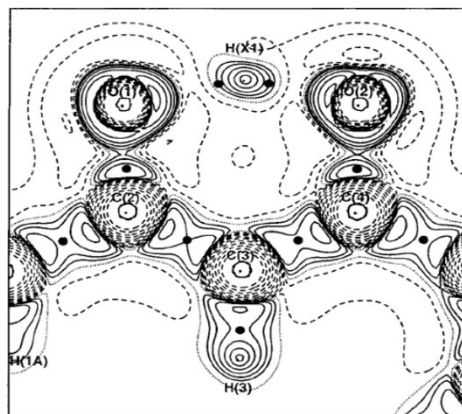
QTAIM approach

Madsen GKH, Iversen BB, Larsen FK, Kapon M, Reisner GM, Herbstein FH. Topological Analysis of the Charge Density in Short Intramolecular O-H---O Hydrogen Bonds. Very Low Temperature X-ray and Neutron Diffraction Study of Benzoylacetone. J. Am. Chem. Soc. 1998; 120:10040-10045.
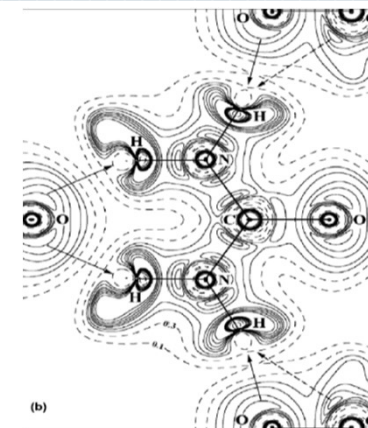
ELF approach

Tsirelson V, Stash A. Determination of the electron localization function from electron density. Chem. Phys. Lett. 2002; 142: 142-148.
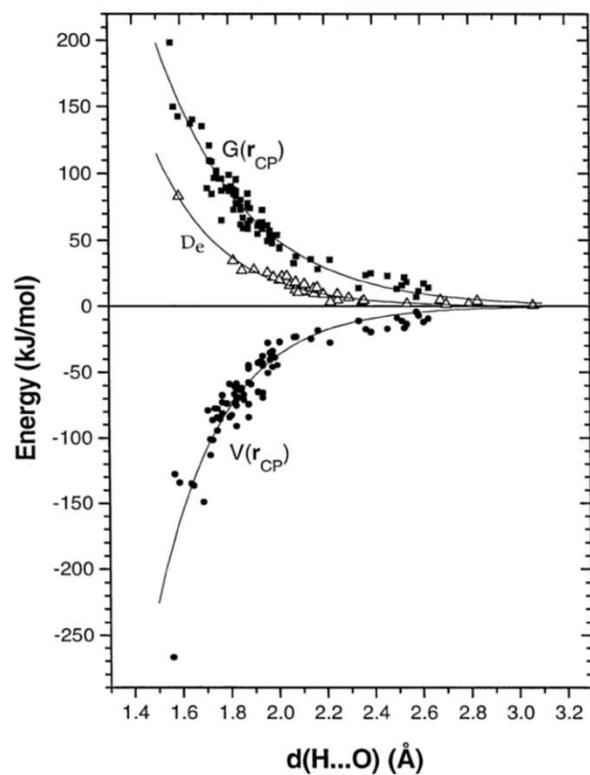
A kind of structure correlation with charge density results (from multipolar model expansions)

Same results using a promolecular approach (spherical atom densities)

Espinosa E, Molins E, Lecomte C. Hydrogen bond strengths revealed by topological analyses of experimentally observed electron densities. Chem. Phys. Lett. 1998; 285:170–173

Spackman M. Hydrogen bond energetics from topological analysis of experimental electron densities: Recognising the importance of the promolecule. Chem. Phys. Lett. 1999; 301:425-429
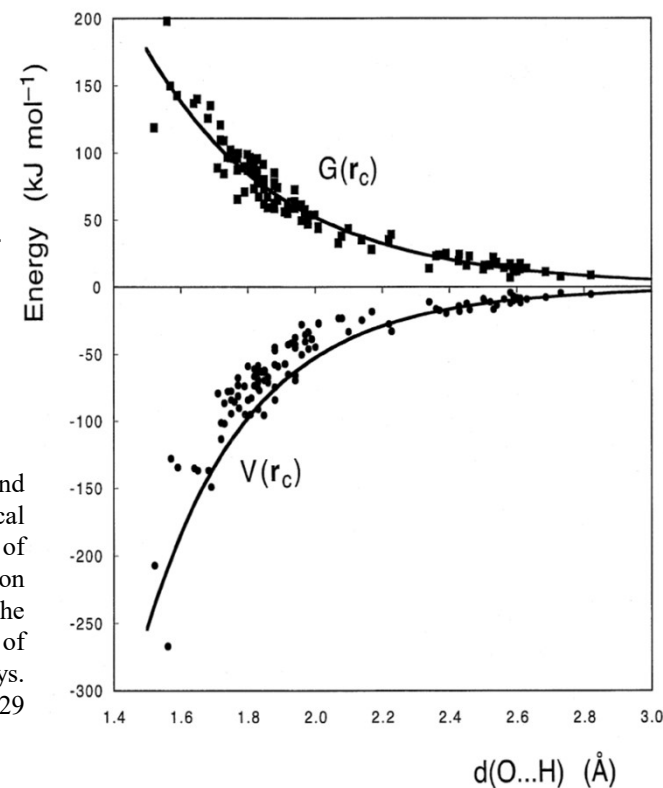
CHARGE and SPIN DENSITY

By R. J. Weiss

SPECIFICATIONS—US ARMY TANK—JULY 2064
. . . medium tank, 4 passenger, armour plated steel, maximum speed 120 mph . . . .

Wave functions must be specified to within 1% at all points in the atomic polyhedra. One electron observables to be evaluated . . . .

of about one percent. However, s only been achieved in a very li cases, such as the inert gases, Ne, and the solids, Al, Fe, Cr, Cu, Ge. The problems encountered i measured structure factors into have not been adequately solved

The above excerpt might be taken from specifications for an Army tank in the year 2064 since high-speed computers may then be capable of calculating all pertinent observables (strength, hardness, thermal conductivity, etc.) from the wave functions. However, projected military require-

Weiss RJ. Charge and Spin Density. Physics Today 1965; **18**: 43-44.

Wavefunction models: a molecular wavefunctions adjusted to reproduce the measured X-ray diffraction

$$\hat{H}\psi = E\psi \qquad \rho(\mathbf{r}) \div |\psi(\mathbf{r})|^2$$

Approximated Hamiltonian

$$\hat{H}'\psi' = E\psi' \qquad \hat{H} = \hat{H}' + \hat{H}_{err}$$

X-ray Determination of Electron Distribution

Weiss, R J

Note: This is not the actual book cover
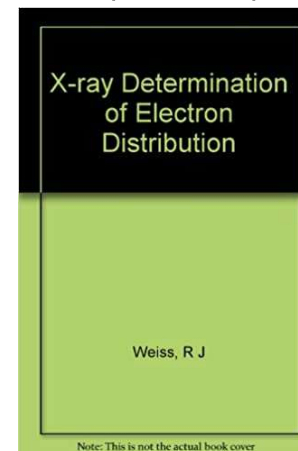
Weiss RJ. X-ray determination of Electron Distributions. North-Holland Publishing Company. Amsterdam. 1966.

Wavefunction models: a molecular wavefunctions adjusted to reproduce the measured X-ray diffraction

Jayatilaka D. Wave Function for Beryllium from X-Ray Diffraction Data. Phys. Rev. Lett. 1998; 80: 798–801.

$$\hat{J}\psi_{XC} = E_{XC}\psi_{XC} \qquad \hat{J} = \hat{H}'[\psi'] + \lambda\left(\chi^2[\psi'] - \Delta\right)$$

$$\chi^2 = \frac{1}{N_r - N_p}\sum_{\mathbf{H}}\frac{\left|\eta\left(F_{\mathbf{H}}^{calc}\right)^2 - \left(F_{\mathbf{H}}^{target}\right)^2\right|}{\left[\sigma\left(F_{\mathbf{H}}^{target}\right)\right]^2}$$

Wavefunction models: Hirshfeld atom refinement

$$\hat{H}'\psi' = E\psi' \Longrightarrow \rho(\mathbf{r}) \div |\psi'(\mathbf{r})|^2 \Longrightarrow \rho(\mathbf{r}) = \sum_i \rho_i(\mathbf{r})$$

$$\Longrightarrow f_i(\mathbf{k}) \Longrightarrow \mathbf{F}(\mathbf{k}) = \sum_i f_i(\mathbf{k})T_i(\mathbf{k})e^{-i\mathbf{k}\cdot\mathbf{r}_i}$$

Jayatilaka D, Dittrich B. X-ray structure refinement using aspherical atomic density functions obtained from quantum-mechanical calculations. Acta Cryst. 2008; A64: 383-393

Density matrix from X-ray diffraction experiments. N-representability problem

Clinton W, Massa L. Determination of the Electron Density Matrix from X-Ray Diffraction Data Phys. Rev. Lett. 1972; 29: 1363-1366.

Density matrix models: Refinement of atomic expansion against Compton profiles

$$\Gamma(\mathbf{r}',\mathbf{r}) = \sum_a \Gamma_a(\mathbf{r}',\mathbf{r}) + \sum_{a,b}\Gamma_{ab}(\mathbf{r}',\mathbf{r})$$

Gillet J-M. Determination of a one-electron reduced density matrix using a coupled pseudo-atom model and a set of complementary scattering data. Acta Cryst. 2007; A63: 234-238.

Wavefunction models: Stewart atom refinement

Stewart atoms are the unique nuclear-centered spherical functions whose sum best fits a molecular electron density in a least-squares sense.

4. Wavefunction from experiment
First attempt of X-ray wavefunction refinement

$$\psi = \det|\varphi_i|_{i=1,N_{molorb}}$$

$$\varphi_i = \sum_{\mu=1}^{N_{atorb}} c_{i,\mu}\chi_\mu \qquad \text{MO-LCAO}$$

$$\rho(\mathbf{r}) = \sum_{\mu=1}^{N_{atorb}} \sum_{\nu=1}^{N_{atorb}} \sum_{i=1}^{N_{molorb}} n_i c_{i,\mu} c_{i,\nu} \chi_\mu \chi_\nu = \sum_{\mu=1}^{N_{atorb}} \sum_{\nu=1}^{N_{atorb}} P_{\mu\nu} \chi_\mu \chi_\nu$$

Population coefficients   Atomic orbital products

Coppens P, Csonka LN, Willoughby TV. Electron Population Parameters from Least-Squares Refinement of X-ray Diffraction Data. Science. 1970; 167: 1126-1128
Coppens P, Willoughby TV, Csonka LN. Electron Population Analysis of Accurate Diffraction Data. I. Formalisms and Restrictions. Acta Cryst. 1971; A27: 248-256
Coppens P, Pautler D, Griffin JF. Electron Population Analysis of Accurate Diffraction Data. II Application of One-Center Formalisms to Some Organic and Inorganic Molecules. J. Am. Chem. Soc. 1971; 93: 1051-1058.

Problem: χ_μ and χ_ν may be centered on two different atoms (two-center terms).

$$\mathbf{F}(\mathbf{k}) = \sum_j f_j(\mathbf{k}) T_j(\mathbf{k}) e^{i\mathbf{k}\cdot\mathbf{r}}$$

POLITECNICO MILANO 1863

4. Wavefunction from experiment
X-ray Atomic Orbital Model, X-ray Molecular Orbital Model,
Valence Orbital Model, Molecular Orbital Occupation Number

$$\{\mathbf{F}(\mathbf{k})\}_{|\mathbf{k}| \le k_{max}} \longleftarrow \rho(\mathbf{r}) = \sum_{\mu=1}^{N_{atorb}} \sum_{\nu=1}^{N_{atorb}} \sum_{i=1}^{N_{molorb}} n_i c_{i,\mu} c_{i,\nu} \chi_\mu \chi_\nu = \sum_{\mu=1}^{N_{atorb}} \sum_{\nu=1}^{N_{atorb}} P_{\mu\nu} \chi_\mu \chi_\nu$$

XAO: atomic states, one-center terms

XMO: one-center and two-center terms (with conditions of orthonormal set of MOs)

MOON: refinement of occupation numbers of canonical or natural MOs

VOM: refinement of valence shell orbital overlap population (within Ligand Field Theory)

Tanaka, K., Makita, R., Funahashi, S., Komori, T. & Win, Z. (2008). X-ray atomic orbital analysis. I. Quantum mechanical and crystallographic framework of the method. Acta Cryst.; B64: 437-449.

Tanaka, K. X-ray molecular orbital analysis. I. Quantum mechanical and crystallographic framework. Acta Cryst. 2018; A74: 345-356.

Hibbs, D. E.; Howard, S. T.; Huke, J. P.; Waller, M. P. A new orbital-based model for the analysis of experimental molecular charge densities: an application to (Z)-N-methyl-C-phenylnitrone. Phys. Chem. Chem. Phys. 2005; 7: 1772-1778.

Figgis BN, Reynolds PA, Williams GA. Spin-density and bonding in the $[CoCl_4]^{2-}$ ion in Cs_3CoCl_5. 2. Valence electron-distribution in the $CoCl_4^{2-}$ ion. J. Chem. Soc. Dalton Trans. 1980: 2339-2347.

5. Electron charge and/or spin density from experiment

$$\rho_{molecule}(\mathbf{r}) = \rho_{promolecule}(\mathbf{r}) + \Delta\rho(\mathbf{r}) = \sum_{i=1}^{N_{at}} \rho_{i,sph}(\mathbf{r} - \mathbf{R}_i) + \sum_{i=1}^{N_{at}} \Delta\rho_i(\mathbf{r} - \mathbf{R}_i) = \sum_{i=1}^{N_{at}} \rho_{i,asph}(\mathbf{r} - \mathbf{R}_i)$$

Charge Density:
Kurki-Suonio K, Meisalo V. Non-spherical deformations of the ions in Fluorite. J. Phys. Soc. Jap. 1966; 21: 122–126.
Stewart RF. Electron population analysis with rigid pseudoatoms. Acta Cryst. 1976; A32: 565-574
Hirshfeld FL. Deformation Density refinement program. Isr. J. Chem. 1977; 16: 226-229
Hansen NK, Coppens P. Electron Population Analysis of Accurate Diffraction Data. 6. Testing Aspherical Atom Refinements on Small-Molecule Data Sets. Acta Cryst. 1978; A34: 909-921.

Spin Density:
Bonnet M, Delapalme A, Fuess H, Becker P. Polarized neutron study of covalency effects in yttrium iron garnet. J. Phys. Chem. Solids. 1979; 40: 863-876.
Becker P, Coppens P. About the simultaneous interpretation of charge and spin density data. Acta Cryst. 1985; A41: 177-182.

POLITECNICO MILANO 1863

Finally, there is a still deeper application of the X-ray analysis, to the structure of the atom itself. Since the wavelength of the X-rays is less than the "atomic diameter", as it is somewhat vaguely termed, and since the rays are presumably diffracted by the electrons in the atom, we ought to be able to get some idea of the distribution of these electrons in the same way that we draw conclusions as to the grouping of the atoms. Interference between the waves scattered by the electrons must take place. In order to study this question, a much closer analysis of the mechanism of X-ray reflexion must be made. Many workers have attacked this problem, amongst them Darwin in England, Debye in Germany, Compton in America. We have been trying to make some accurate quantitative determinations of the strength of X-ray reflection, the object in view being the measurement of the amount of radiation scattered by an atom in all directions when an X-ray beam passes over it. The whole subject bristles with difficulties, and the assumptions on which the theory of reflexion rests have not been exhaustively proved. On the other hand there seems to be a prospect that the method will prove a valid way of testing various models proposed for the atom, since the way, in which these models should diffract the rays, can be calculated, and compared with that which is actually observed.

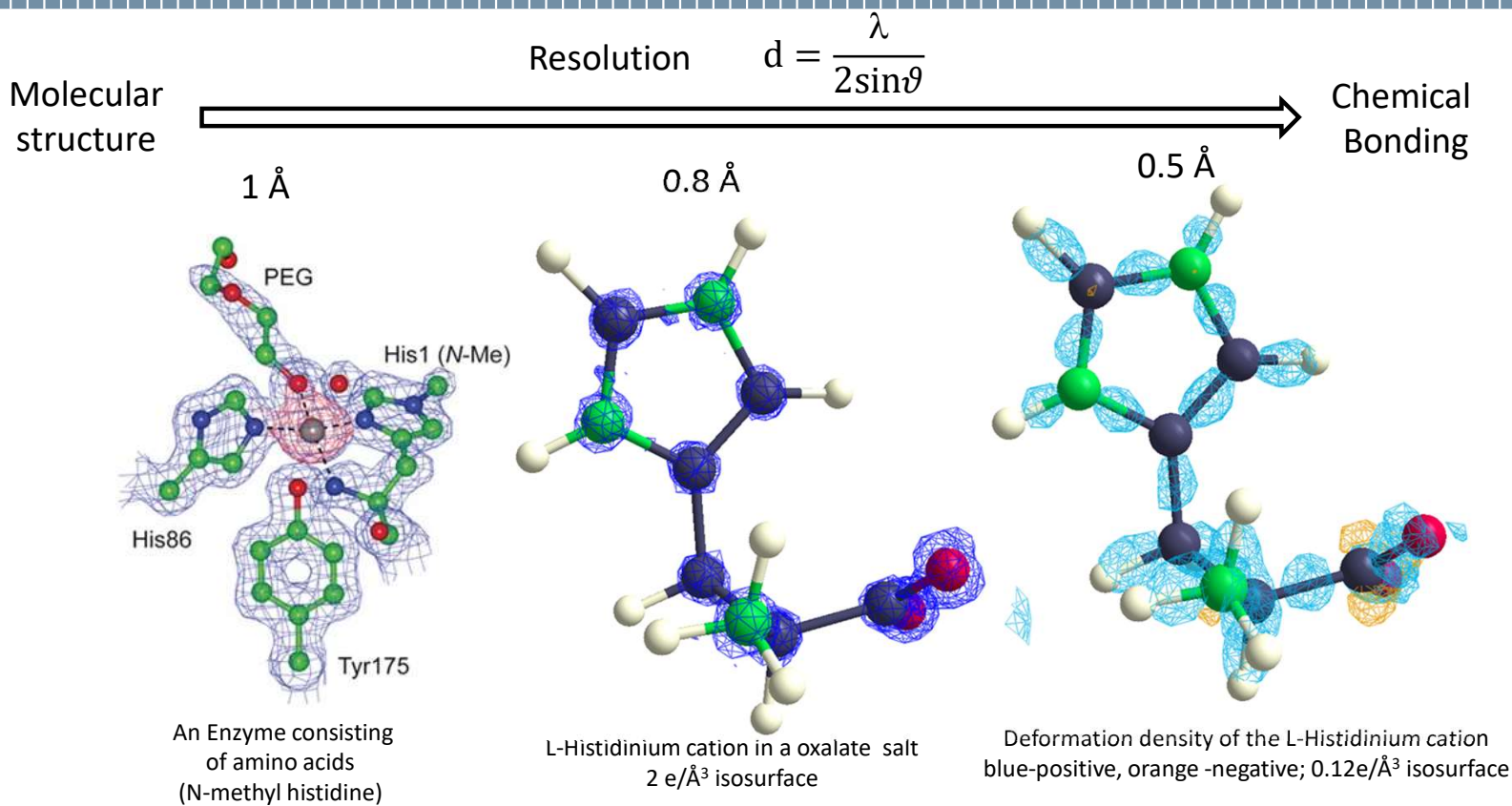Bragg WL. The diffraction of X-rays by crystals. Nobel Lecture. 1922; 370-382.

State of the Art

Resolution $\quad d = \dfrac{\lambda}{2\sin\vartheta}$

Molecular structure $\longrightarrow$ Chemical Bonding

1 Å

0.8 Å

0.5 Å

An Enzyme consisting
of amino acids
(N-methyl histidine)

L-Histidinium cation in a oxalate salt
2 e/Å^3 isosurface

Deformation density of the L-Histidinium cation
blue-positive, orange -negative; 0.12e/Å^3 isosurface

Non spherical atomic form factors

McWeeny R. X-ray scattering by aggregates of bonded atoms. I. Analytical approximations in singe-atom scattering. Acta Cryst. 1951; 4: 513-519;
McWeeny R. X-ray scattering by aggregates of bonded atoms. II. The effect of the bonds: with an application to H_2. Acta Cryst. 1952; 5: 463-468;
McWeeny R. X-ray scattering by aggregates of bonded atoms. III. The bond scattering factor: simple methods of approximation in the general case. Acta Cryst. 1953; 6: 631-637;
McWeeny R. X-ray scattering by aggregates of bonded atoms. IV. Applications to the carbon atom. Acta Cryst. 1954; 7: 180-185.

$$\rho_{at,asph}(\mathbf{r}) \longrightarrow f_{at,asph}(\mathbf{k})$$
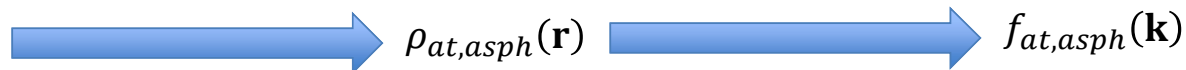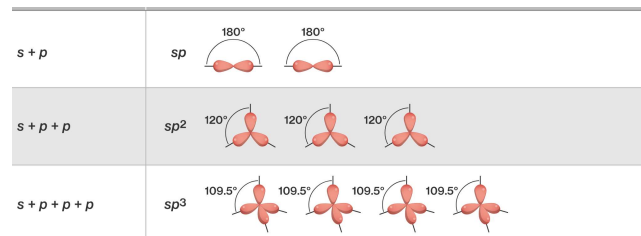
Generalized atomic form factors

Dawson B. Aspherical Atomic Scattering Factors in Crystal Structure Refinement I. Coordinate and Thermal Motion Effects in a Model Centrosymmetric System. Acta Cryst. 1964; 17: 990-996;
Dawson B. A general structure factor formalism for interpreting accurate X-ray and neutron diffraction data. Proc. Roy. Soc. A, 1967a, 298, 255-263;
Dawson B. The Covalent Bond in Diamond. Proc. Royal. Soc. London A. 1967b; 298: 264-288.

Stewart RF, Davidson ER, Simpson WT. Coherent X-ray scattering for the hydrogen atom in the hydrogen molecule. J. Chem. Phys. 1965, 42: 3175-3187.
Stewart RF. Generalized x-ray scattering factors. J. Phys. Chem. 1969, 51: 4569-4577;
Stewart RF, Bentley J, Goodman B. Generalized x-ray scattering factors in diatomic molecules. J. Chem. Phys., 1975, 63: 3786-3793;

$$\psi = \det|\varphi_i|_{i=1,N_{molorb}} \longrightarrow \sum_{\mu=1}^{N_{atorb}} \sum_{\nu=1}^{N_{atorb}} P_{\mu\nu}\chi_\mu\chi_\nu \longrightarrow f_{\mu\nu} \longrightarrow \rho_{at,asph}(\mathbf{r}) \longrightarrow f_{at,asph}(\mathbf{k})$$
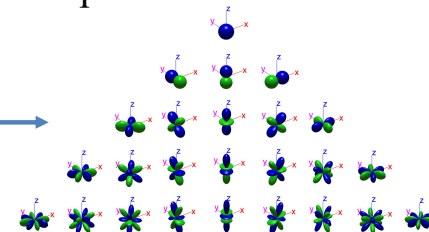
$$\rho_{molecule}(\mathbf{r}) = \rho_{promolecule}(\mathbf{r}) + \Delta\rho(\mathbf{r}) = \sum_{i=1}^{N_{at}} \rho_{i,sph}(\mathbf{r} - \mathbf{R}_i) + \sum_{i=1}^{N_{at}} \Delta\rho_i(\mathbf{r} - \mathbf{R}_i) = \sum_{i=1}^{N_{at}} \rho_{i,asph}(\mathbf{r} - \mathbf{R}_i)$$

spherical harmonics

$$\rho_{i,asph}(\boldsymbol{r}) = P_{i,\text{core}}\rho_{i,core}(\boldsymbol{r}) + \sum_{l=0,}^{l_{max}} \left[R_{i,l}(\zeta,\boldsymbol{r}) \sum_{m=0,l} P_{i,lm\pm} y_{lm\pm}(\boldsymbol{r}/r) \right]$$

Stewart RF. Electron population analysis with rigid pseudoatoms. Acta Cryst. 1976; A32: 565-574
Stewart RF. Electron population analysis with generalized x-ray-scattering factors - higher multipoles. J. Chem. Phys. 1973; 58: 1668-1676.
Program: VALRAY

$$\rho_{i,asph}(\boldsymbol{r}) = \rho_{i,core}(\boldsymbol{r}) + P_{i,valence}\kappa_i^3 \rho_{i,valence}(\kappa_i \boldsymbol{r}) + \sum_{l=0,}^{l_{max}} \left[{\kappa'}_i^3 R_{i,l}(\kappa'_l \boldsymbol{r}) \sum_{m=0,l} P_{i,lm\pm} y_{lm\pm}(\boldsymbol{r}/r) \right]$$

Hansen NK, Coppens P. Electron Population Analysis of Accurate Diffraction Data. 6. Testing Aspherical Atom Refinements on Small-Molecule Data Sets. Acta Cryst. 1978; A34: 909-921.
Programs: MOLLY, XD, MoPro, WinXPRO, JANA

$$\rho_i(\boldsymbol{r}) = P_{i,core}\kappa_{i,core}^3\rho_{i,core}(\boldsymbol{r}) + P_{i,valence}\kappa_{i,valence}^3\rho_{i,valence}(\boldsymbol{r})$$

$$+ \sum_{l=0,}^{l_{max}}\left[\kappa'^3_{i,core}R_{i,core,l}(\kappa'_l\boldsymbol{r})\sum_{m=0,l}P_{i,core,lm\pm}y_{lm\pm}(\boldsymbol{r}/r)\right]$$

$$+ \sum_{l=0,}^{l_{max}}\left[\kappa'^3_{i,valence}R_{i,valence,l}(\kappa'_l\boldsymbol{r})\sum_{m=0,l}P_{i,valence,lm\pm}y_{lm\pm}(\boldsymbol{r}/r)\right]$$

Fischer A, Tiana D, Scherer W, Batke K, Eickerling G, Svendsen H, Bindzus N, Iversen BB. Experimental and Theoretical Charge Density Studies at Subatomic Resolution. J. Phys. Chem. A. 2011; 115:13061-13071.

Bindzus N, Straasø T, Wahlberg N, Becker J, Bjerg L, Lock N, Dippel A-C, Iversen BB. Experimental determination of core electron deformation in diamond. Acta Cryst. 2014; A70: 39-48
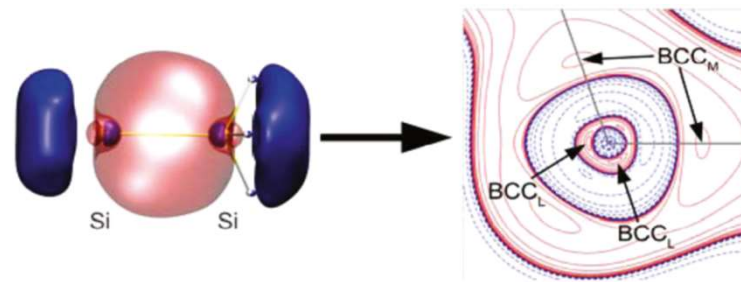
POLITECNICO MILANO 1863

By combination of X-ray diffraction, Neutron diffraction and Polarized neutron diffraction:

$$\rho_i(\mathbf{r}) = \rho_{i,core}(\mathbf{r}) + \kappa_{i,valence}^3 \rho_{i,valence}(\mathbf{r}) \left(P_{i,val}^\alpha + P_{i,val}^\beta\right) + \sum_{l=0,}^{l_{max}} \left[\kappa_i'^3 R_{i,l}(\kappa_l'\mathbf{r}) \sum_{m=0,l} \left(P_{i,lm\pm}^\alpha + P_{i,lm\pm}^\beta\right) y_{lm\pm}(\mathbf{r}/r)\right]$$

Deutsch M, Claiser N, Pillet S, Chumakov Y, Becker P, Gillet JM, Gillon B, Lecomte C, Souhassou M. Experimental deter-mination of spin-dependent electron density by joint refinement of X-ray and polarized neutron diffraction data. Acta Cryst. 2012; A68: 675-686;
Deutsch M, Gillon B, Claiser N, Gillet JM, Lecomte C, Souhassou M. First spin-resolved electron distributions in crystals from combined polarized neutron and X-ray diffraction experiments. IUCrJ. 2014; 1: 194-199.
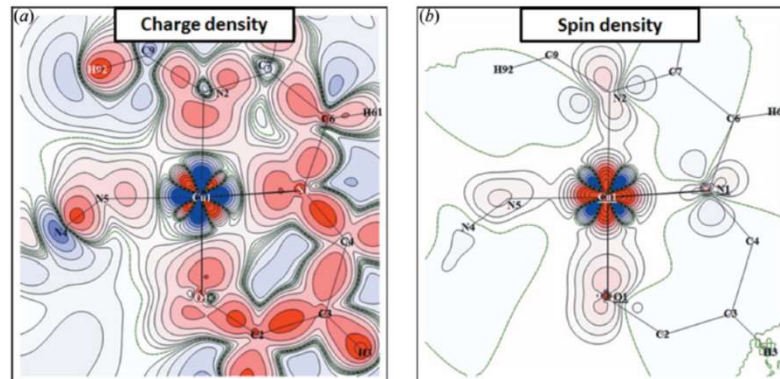
$$\rho_{i,asph}(\mathbf{r}) = \rho_{i,core}(\mathbf{r}) + P_{i,valence}\kappa_i^3 \rho_{i,valence}(\kappa_i \mathbf{r}) + \sum_{l=0,}^{l_{max}} \left[{\kappa'}_i^3 R_{i,l}(\kappa'_l \mathbf{r}) \sum_{m=0,l} P_{i,lm\pm} y_{lm\pm}(\mathbf{r}/r) \right]$$

Averaged values from sets of experimental measurements (ELMAM)

Pichon Pesme V, Lecomte C, Lachekar H. On Building A Data-Bank Of Transferable Experimental Electron-Density Parameters - Application To Polypeptides. J. Phys. Chem. 1995; 99: 6242-6250;

Domagała S, Fournier B, Liebschner D, Guillot B, Jelsch C. An improved experimental databank of transferable multipolar atom models – ELMAM2. Construction details and applications. Acta Cryst. 2012; A68: 337-351

Averaged values from sets of theoretical calculations (UBDB, UBDB2)

Dominiak PM, Volkov A, Li X, Messerschmidt M, Coppens P. A theoretical databank of transferable aspherical atoms and its application to electrostatic interaction energy calculations of macromolecules. J. Chem. Theo. Comp. 2007; 3: 232-247;

Jarzembska KN, Dominiak PM. New version of the theoretical databank of transferable aspherical pseudoatoms, UBDB2011 - Towards nucleic acid modelling. Acta Cryst. 2012; 68: 139-147;

Kumar P, Bojarowski SA, Jarzembska KN, Domagała S, Vanommeslaeghe K, Mackerell AD, Dominiak PM. A comparative study of transferable aspherical pseudoatom databank and classical force fields for predicting electrostatic interactions in molecular dimers. J. Chem. Theor. Comput. 2014; 10: 1652-1664.

Values from a specific theoretical calculation (INVARIOM)

Dittrich B, Hubschle C, B, Luger P, Spackman MA. Introduction and validation of an invariom database for amino-acid, peptide and protein molecules. Acta Cryst 2006; A62: 1325-133

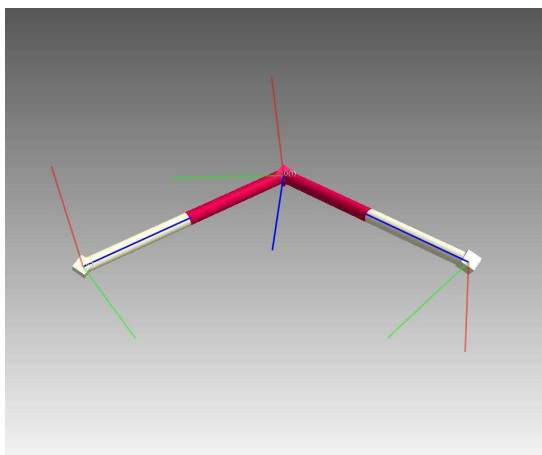$P_{i,valence}$ $P_{i,lm\pm}$ κ κ' constrained to

they are not refined

- Refinement of (macro)molecular crystals for which a sufficient data quality cannot be obtained.

- Evaluation of electrostatic properties using molecular geometries (determined with traditional refinements or with multipole constrained refinements)

The local coordinate system, fundamental
for the multipole transferability

Domagała S, Fournier B, Liebschner D, Guillot B, Jelsch C. An improved experimental databank of transferable multipolar atom models – ELMAM2. Construction details and applications. Acta Cryst., 2012; A68: 337-351

Ernst M, Dos Santos LHR, Krawczuk, Macchi P. Towards a generalized database of atomic polarizabilities. In Understanding Intermolecular Interactions in the Soldi State: approaches and techniques. Ed. D. Chopra. The Royal Society of Chemistry. Monographs in Supramolecular Chemistry. 2019; 26: 211-242.

The Schrodinger Equation

$$H\psi = E\psi \qquad\qquad\longrightarrow\qquad\qquad J[\psi] = E[\psi] + {\color{red}\lambda}\chi^2[\psi]$$

$$\chi^2 = \frac{1}{N_r - N_p} \sum_{\boldsymbol{h}} \frac{\left(\eta\left|F_{\boldsymbol{h}}^{calc}\right| - \left|F_{\boldsymbol{h}}^{exp}\right|\right)^2}{\sigma_{\boldsymbol{h}}^2}$$

X-ray Determination of Electron Distribution

Weiss, R J

Note: This is not the actual book cover
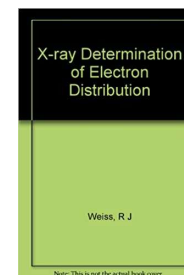
This approach is the realization of Weiss' dream

Jayatilaka, D. Wave Function for Beryllium from X-Ray Diffraction Data. Phys. Rev. Lett. 1988; 80: 798-801.
Jayatilaka, D.; Grimwood, D. J. Wavefunctions Derived from Experiment. I. Motivation and Theory. Acta Crystallogr., Sect. A 2001; 57: 76−86.
Grimwood, D. J.; Jayatilaka, D. Wavefunctions Derived from Experiment. II. A Wavefunction for Oxalic Acid Dihydrate. Acta Crystallogr., Sect. A 2001; 57: 87−100.
Bytheway, I.; Grimwood, D. J.; Jayatilaka, D. Wavefunctions Derived from Experiment. III. Topological Analysis of Crystal Fragments. Acta Crystallogr., Sect. A 2002; 58: 232−243.
Bytheway, I.; Grimwood, D. J.;, Figgis, B. N.; Chandler, G. S.; Jayatilaka, D. Wavefunctions Derived from Experiment. IV. Investigation of the Crystal Environment of Ammonia. Acta Crystallogr., Sect. A 2002; 58: 244−251.

The wavefunction ψ is *molecular* (or supramolecular) but not *crystalline*
Thus, the restraint to the experimental data includes *both* the effects of the crystal field and all those electronic interactions which are not considered in the Hamiltonian (e.g. electron correlation, if using Hartree-Fock method, relativistic effects, if using a non relativistic approach, etc.)
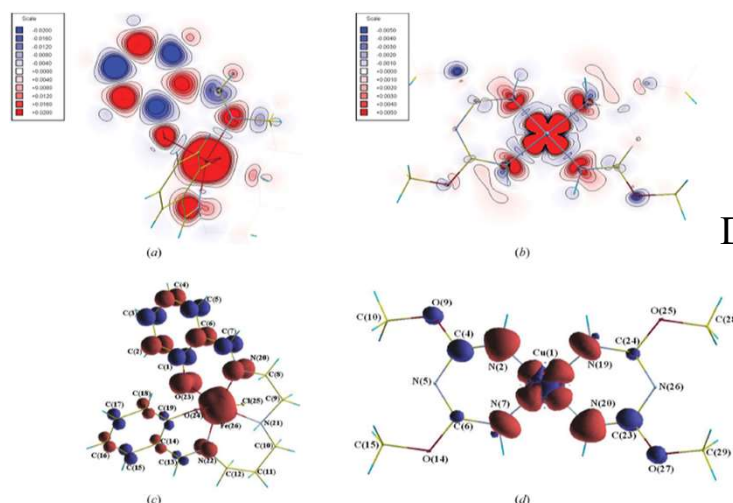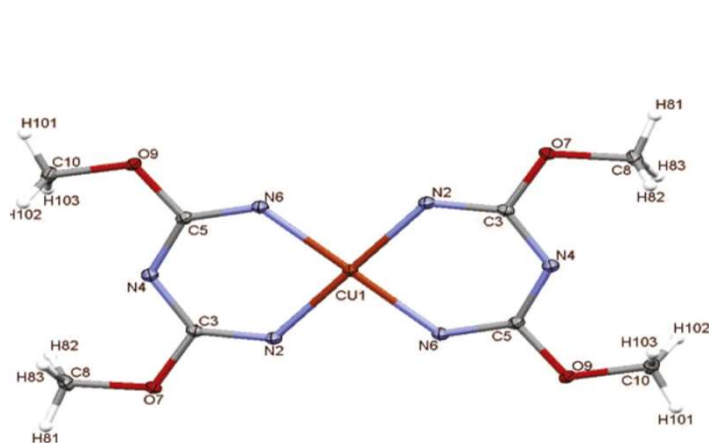
Ernst, M.; Genoni, A.; Macchi, P. Analysis of crystal field effects and interactions using X-ray restrained ELMOs. J. Mol. Struct. 2020; 1209: 127975.

Genoni, A.; Dos Santos, L. H. R.; Meyer, B.; Macchi, P. Can X-ray constrained Hartree-Fock wavefunctions retrieve electron correlation? IUCrJ 2017; 4: 136-146.

POLITECNICO MILANO 1863

Douglas Kroll Hess Hamiltonian

Bučinský, L.; Biskupič, S.; Jayatilaka, D. Study of the picture change error at the 2nd order Douglas Kroll Hess level of theory. Electron and spin density and structure factors of the Bis[bis(methoxycarbimido) aminato] copper (II) complex. Chem. Phys. 2012; 395: 44–53.

Bučinský, L.; Jayatilaka, D.; Grabowsky, S. Importance of Relativistic Effects and Electron Correlation in Structure Factors and Electron Density of Diphenyl Mercury and Triphenyl Bismuth. J. Phys. Chem. A 2016; 120: 6650-6669.

Bučinský, L.; Jayatilaka, D.; Grabowsky, S. Relativistic Quantum Crystallography of Diphenyl and Dicyano Mercury. Theoretical Structure Factors and Hirshfeld Atom Refinement. Acta Crystallogr., Sect. A 2019; 75: 705–717.

Hudák, M.; Jayatilaka, D.; Peraínova, L.; Biskupic, S.; Kozísek, J.; Bučinský, L. X-ray Constrained Unrestricted Hartree−Fock and Douglas−Kroll−Hess Wavefunctions. Acta Crystallogr., Sect. A 2010; 66: 78−92.

1. Standard electron density models and beyond
Extremely localized molecular orbital wavefunctions from X-ray diffraction

$$J[\psi] = E[\psi] + \lambda\chi^2[\psi]$$

$$\psi = \sum_j C_j \, \psi_{ELMO,j}$$

Strictly localized molecular orbitals

Genoni, A. Molecular Orbitals Strictly Localized on Small Molecular Fragments from X-ray Diffraction Data. J. Phys. Chem. Lett. 2013; 4: 1093-1099.
Genoni, A. X-ray Constrained Extremely Localized Molecular Orbitals: Theory and Critical Assessment of the New Technique. J. Chem. Theory Comput. 2013; 9: 3004-3019

ELMO constrained refinement → Database approach

Meyer, B.; Genoni, A. Libraries of Extremely Localized Molecular Orbitals. 3. Construction and Preliminary Assessment of the New Databanks. J. Phys. Chem. A 2018; 122: 8965−8981.
Macetti, G.; Genoni A. Quantum Mechanics/Extremely Localized Molecular Orbital Method: A Fully Quantum Mechanical Embedding Approach for Macromolecules. J. Phys. Chem. A 2019; 123: 9420-9428.
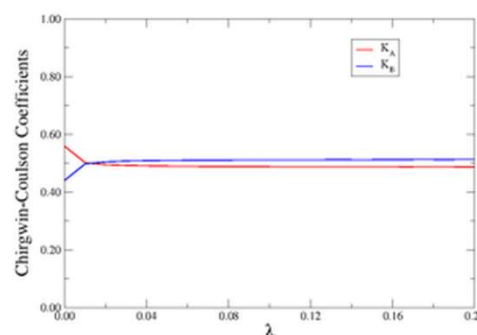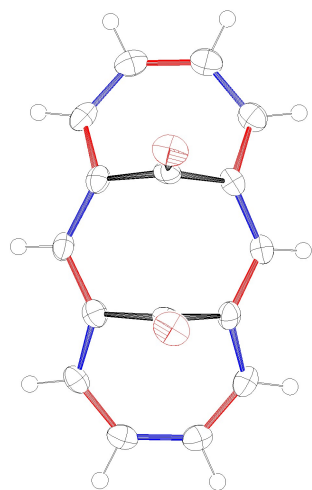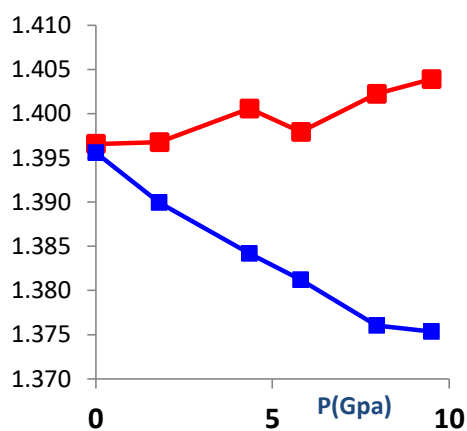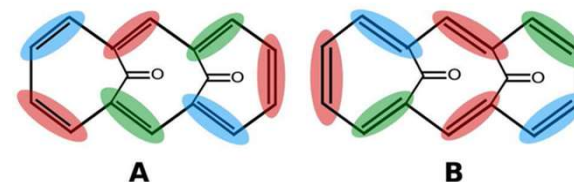
Valence Bond approach

Genoni, A. A first-prototype multi-determinant X-ray constrained wavefunction approach: the X-ray constrained extremely localized molecular orbital-valence bond method. Acta Crystallogr., Sect. A 2017; 73: 312-316.
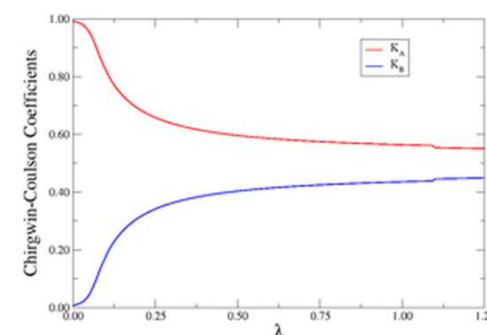
POLITECNICO MILANO 1863

BCA **Pseudo C$_{2v}$**

Casati, N.; Genoni, A.; Meyer, B.; Krawczuk, A.; Macchi, P. Exploring charge density analysis in crystals at high pressure: data collection, data analysis and advanced modelling. Acta Crystallogr., 2017; B73: 584-597.
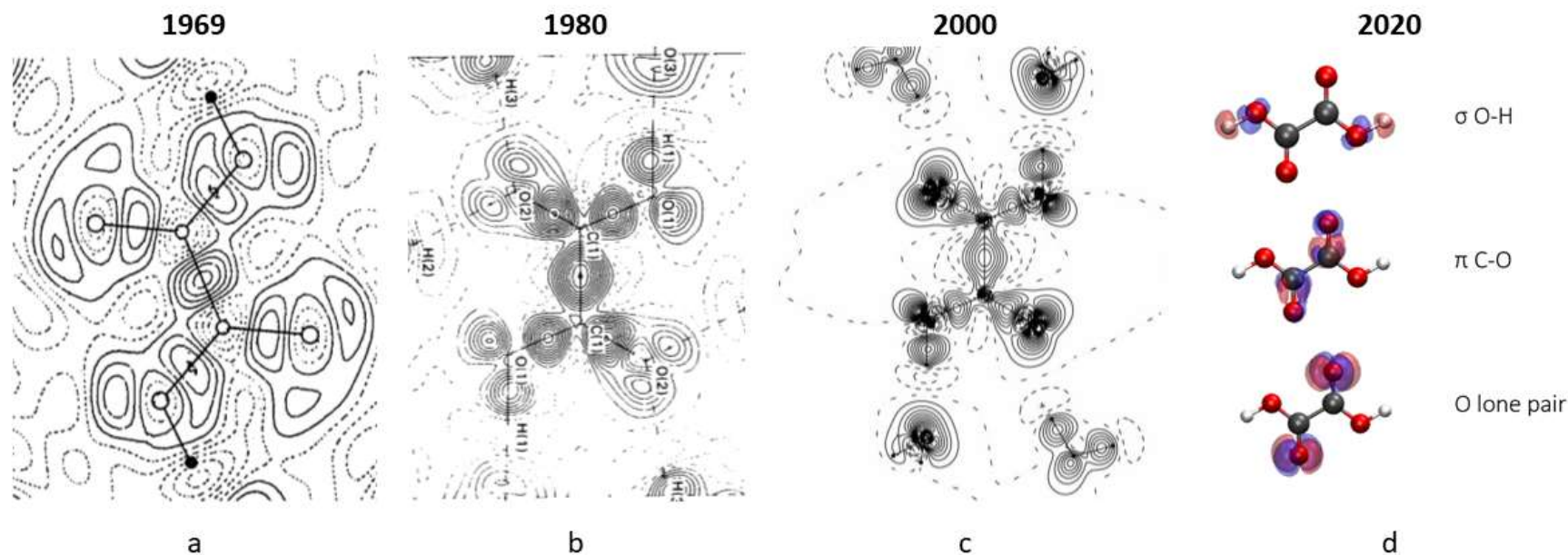

A   B

0.0 GPa   7.7 GPa

Oxalic acid dihydrate in quantum crystallographic studies over the years. (*a*) The experimental *X–N* deformation density map obtained by using the X-ray diffraction structure factors and subtracting the structure factors computed with the independent-atom model from the geometry determined by neutron diffraction (plot modified from Coppens & Sabine, 1969); (*b*) the deformation density map obtained with a multipolar model (from Stevens & Coppens, 1980); (*c*) the deformation density map obtained from the X-ray restrained Hartree–Fock calculation (Grimwood & Jayatilaka, 2001); (*d*) the main molecular orbitals calculated with X-ray restrained extremely localized molecular orbitals (modified from Ernst, Genoni, Macchi, 2020).

POLITECNICO MILANO 1863

$$\rho_j(\mathbf{r}) = \frac{\rho_j^{IAM}(\mathbf{r})}{\sum_i \rho_i^{IAM}(\mathbf{r})} \rho(\mathbf{r})$$

Hirshfeld weighting scheme

Hirshfeld FL. Bonded-atom fragments for describing molecular charge-densities. Theor. Chim. Acta. 1977; 44: 129–138.

$$f_j(\mathbf{S}) = \int \rho_j(\mathbf{r} - \mathbf{R}_j) e^{i\mathbf{k}\cdot\mathbf{r}} d\mathbf{r} = \int \frac{\rho_j^{IAM}(\mathbf{r} - \mathbf{R}_j)}{\sum_i \rho_i^{IAM}(\mathbf{r} - \mathbf{R}_i)} \rho^{theor}(\mathbf{r}) e^{i\mathbf{k}\cdot\mathbf{r}} d\mathbf{r}$$

Jayatilaka D, Dittrich B. X-ray structure refinement using aspherical atomic density functions obtained from quantum-mechanical calculations. Acta Cryst. 2008; A64: 383-393
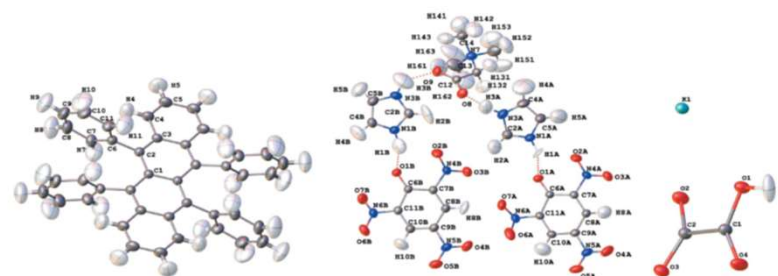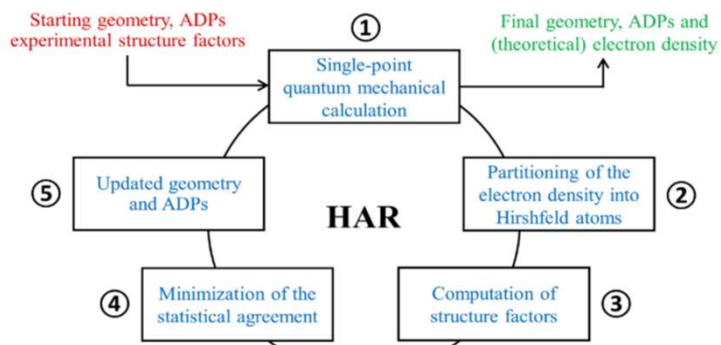
Wieduwilt, E. K.; Macetti, G.; Malaspina, L. A.; Jayatilaka, D.; Grabowsky, S.; Genoni, A. Post-Hartree-Fock methods for Hirshfeld atom refinement: are they necessary? Investigation of a strongly hydrogen-bonded molecular crystal. J. Mol. Struct. 2020; 1209: 127934.
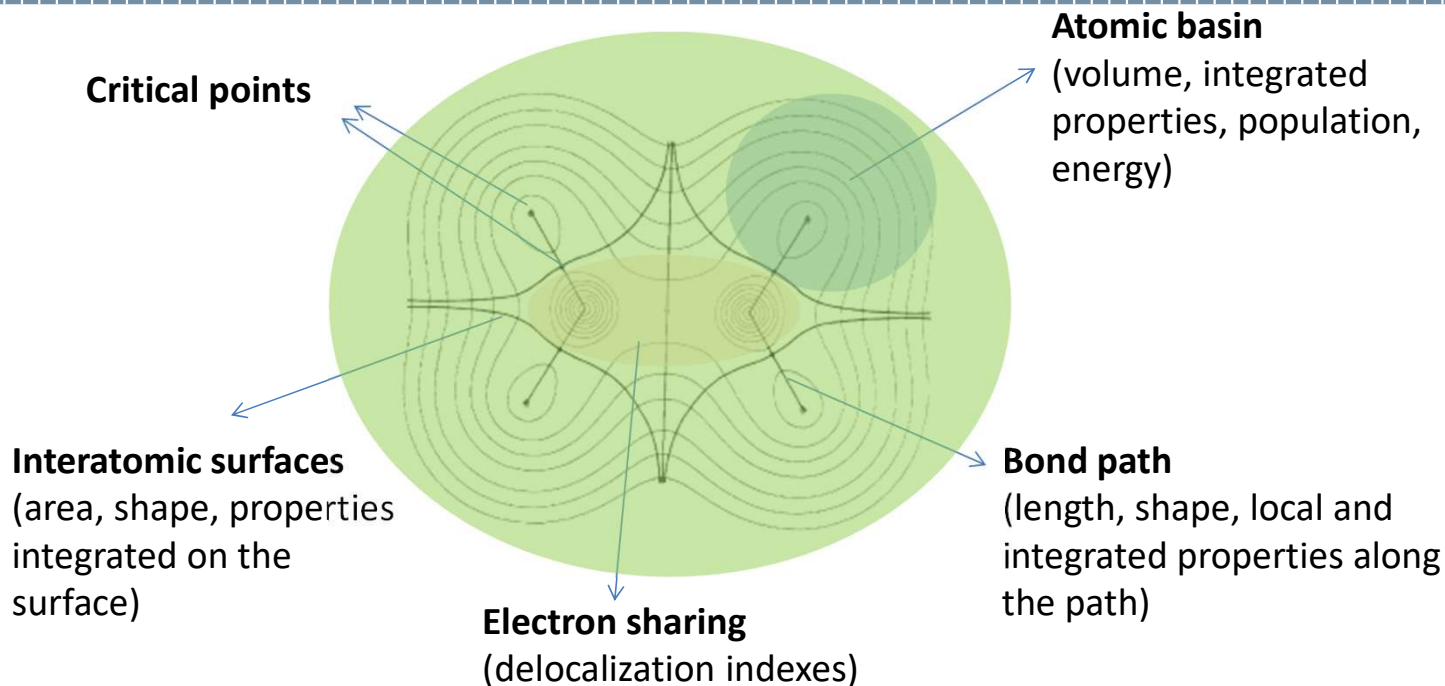
Fugel, M.; Jayatilaka, D.; Hupf, E.; Overgaard, J.; Hathwar, V. R.; Macchi, P.; Turner, J.; Howard, J. A. K.; Dolomanov, O.V.; Puschmann, H.; Iversen, B. B.; Bürgi, H.-B.; Grabowsky, S. Probing the accuracy and precision of Hirshfeld atom refinement with HARt interfaced with Olex2. *IUCrJ* **2018**, *5*, 32-44.
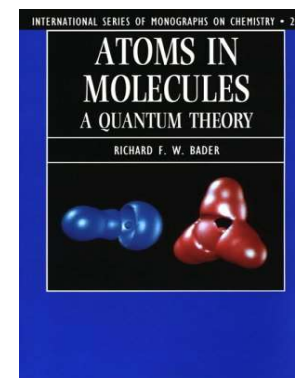
Critical points

Atomic basin
(volume, integrated properties, population, energy)

Interatomic surfaces
(area, shape, properties integrated on the surface)

Electron sharing
(delocalization indexes)

Bond path
(length, shape, local and integrated properties along the path)

Electric potential, field and field gradients to compute interactions with other molecules

R. F. W. Bader Atoms in Molecules : A quantum theory, OUP 1990
P. L. A. Popelier Atoms in Molecules : An Introduction, Pearson, 2000.

POLITECNICO MILANO 1863

$$ELF(\mathbf{r}) = \frac{1}{1 + \chi^2(\mathbf{r})} = \frac{1}{1 + \left(\dfrac{D_\sigma(\mathbf{r})}{D_\sigma^0(\mathbf{r})} \right)^2}$$

$$D_\sigma(\mathbf{r}) = G_\sigma(\mathbf{r}) - \frac{1}{4} \frac{\left| \nabla \rho^\sigma(\mathbf{r}) \right|^2}{\rho^\sigma(\mathbf{r})}$$
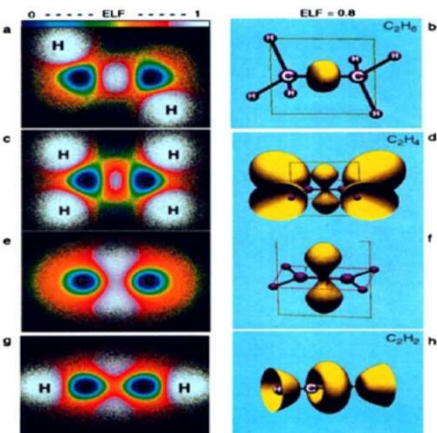
difference between the kinetic energy density $G_\sigma(\mathbf{r})$ (>0) and the bosonic kinetic energy density

$$D_\sigma^0(\mathbf{r}) = \frac{3}{5} \left(6\pi^2 \right)^{\frac{2}{3}} \left(\rho^\sigma(\mathbf{r}) \right)^{\frac{5}{3}}$$
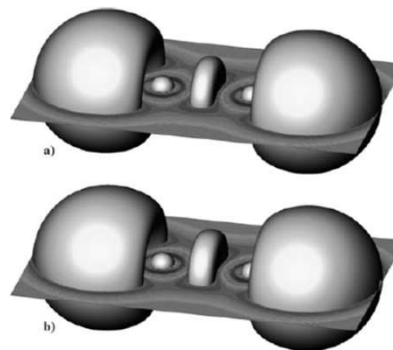
Kinetic Energy of a free electron gas

Becke AD, Edgecombe KE. A simple measure of electron localization in atomic and molecular systems. J. Chem. Phys. 1990; 92: 5397–5403.
Kohout M. A Measure of Electron Localizability. Int. J. of Quant. Chem. 2004; 97: 651–658.

Electron localization function

Electron localizability indicator

From experiment, the Abramov approximation is needed

$$G(\mathbf{r}) \approx G_{DFT}(\mathbf{r}) = \frac{3}{10} \left(3\pi^2 \right)^{\frac{2}{3}} \left(\rho(\mathbf{r}) \right)^{\frac{5}{3}} + \frac{1}{72} \frac{\left[\nabla \rho(\mathbf{r}) \right]^2}{\rho(\mathbf{r})} + \frac{1}{6} \nabla^2 \rho(\mathbf{r})$$

Abramov YA. On the Possibility of Kinetic Energy Density Evaluation from the Experimental Electron-Density Distribution. Acta Cryst. 1997; A53: 264-272.
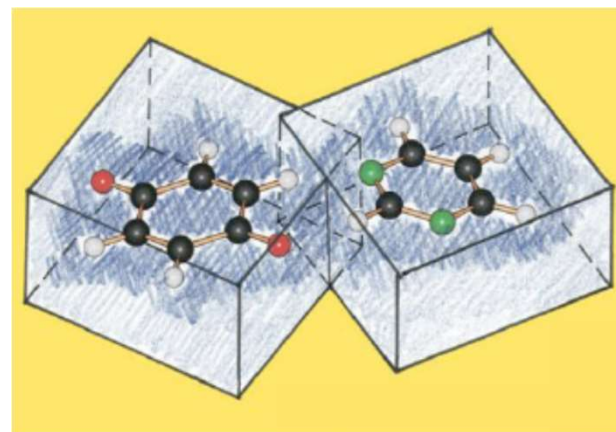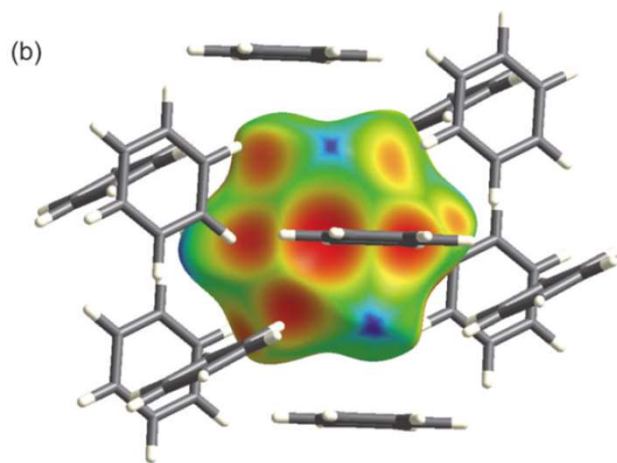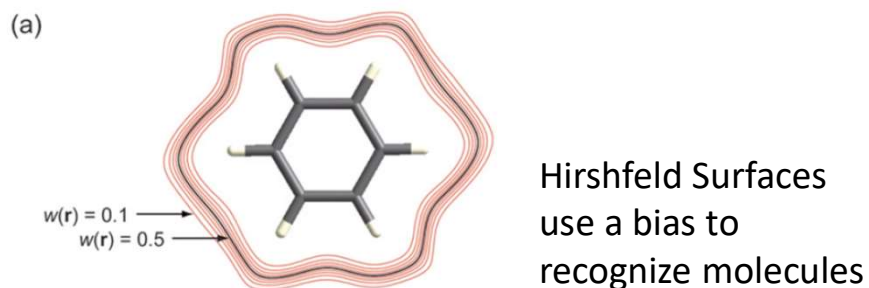
Savin A, Nesper R, Wengert S, Fässler TF. ELF: The Electron Localization Function. Angew. Chem. 1997; 36: 1808-1832.

Kohout M, Pernal K, Wagner F, Grin Y. Electron localizability indicator for correlated wavefunctions. I. Parallel-spin pairs. Theor. Chem. Acc. 2004; 112: 453-459
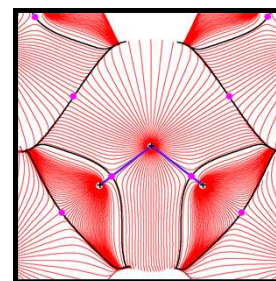
POLITECNICO MILANO 1863

(a)

$w(r) = 0.1$
$w(r) = 0.5$

Hirshfeld Surfaces
use a bias to
recognize molecules

(b)

Gavezzotti A. Calculation of
Intermolecular Interaction Energies by
Direct Numerical Integration over
Electron Densities. I. Electrostatic and
Polarization Energies in Molecular
Crystals. J. Phys. Chem. 2002; 106: 4145-
4154.

PIXEL use a bias to
recognize molecules

QTAIM does not define
molecules in crystals (but a
collection of quantum atoms)

McKinnon JJ, Mitchell AS, Spackman MA. Hirshfeld Surfaces: A New Tool for Visualising
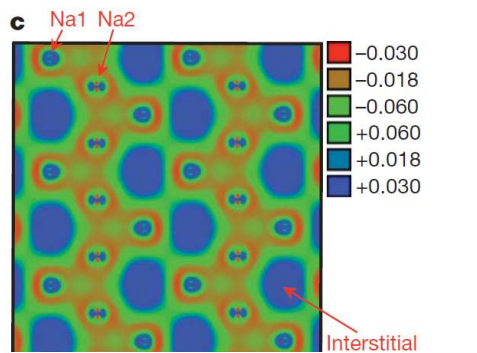and Exploring Molecular Crystals. Chem. Eur. J. 1998; 4: 2136–2141.

R. F. W. Bader Atoms in Molecules : A quantum theory, OUP 1990
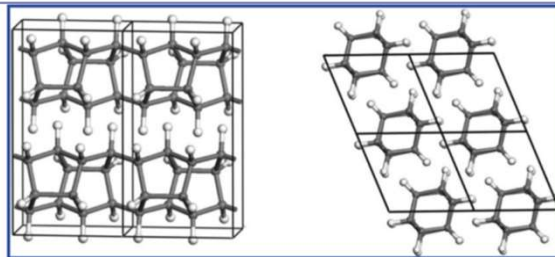
RESEARCH ARTICLE

HIGH-PRESSURE PHYSICS

Observation of the Wigner-Huntington transition to metallic hydrogen

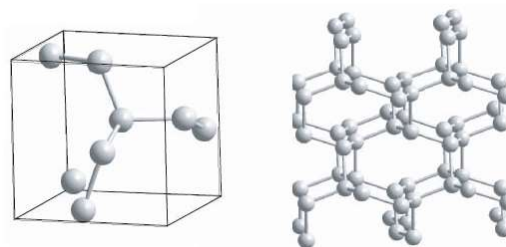Dias, R. P.; Silvera, I. *Science* **2017**, *355*, 715–718

Transparent dense sodium
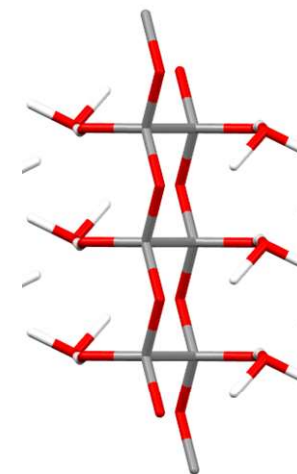Ma *et al. Nature* **2009** *458*, 182-185

Polymerization of benzene

Wen X-D; Hoffmann, R.; Ashcroft, N. W. *J. Am Chem. Soc.* **2011**, *133*, 9023–9035

Single-bonded cubic form of nitrogen

Eremets *et al. Nature Materials* **2004**, *3*, 558-563

Polymerization of oxalic acid

Macchi, Jephcoat, Wilhelm, Casati *manuscript in preparation*

Concluding remarks

Quantum crystallography is the lineal descendent of the science carried out in the early days of X-ray diffraction, when scientists (e.g. Bragg, Debye, Compton) expected to obtain from this technique not only the information about positions of atoms in crystals but also about the actual distribution of electrons around nuclei, by fitting appropriate functions, like the electron density or the electron wavefunction.

Over the time, the interested shifted from atoms to molecules (chemical bonding, polarization) and eventually to crystals, being the *supramolecule par excellence* (J. Dunitz).

Nowadays, the goals are:
- studying the atomic/molecular/crystalline origin of materials properties,
- understanding the interplay between molecules in crystals for crystal engineering
- obtaining information on atomic/molecular excited states to anticipate possible in-crystal reactivity
- extracting information from techniques other than X-ray diffraction (ED, spectroscopy etc.)
- studying the dynamics of crystals
- …… more objectives will be learned during this three day meeting

THANK YOU

and

See You in Prague 2020 ~~2020~~ 2021!!